

# A Robust Snake Implementation; A Dual Active Contour

Steve R. Gunn and Mark S. Nixon

**Abstract**—A conventional active contour formulation suffers difficulty in appropriate choice of an initial contour and values of parameters. Recent approaches have aimed to resolve these problems but can compromise other performance aspects. To relieve the problem in initialization, we use a dual active contour, which is combined with a local shape model to improve the parameterization. One contour expands from inside the target feature, the other contracts from the outside. The two contours are interlinked to provide a balanced technique with an ability to reject “weak” local energy minima.

**Index Terms**—Snakes, active contours, regularization, feature extraction, local shape.

## 1 INTRODUCTION

ACTIVE contours [10], also termed snakes by the nature of their evolution, are a sophisticated approach to contour extraction and image interpretation. They advocate the paradigm that the presence of an edge depends not only on the gradient at a specific point but also on the spatial distribution. Snakes incorporate this global view of edge detection by assessing continuity and curvature, combined with the local edge strength. The principal advantage over other feature extraction techniques is the integration of image data, an initial estimate, desired contour properties and knowledge-based constraints, in a single extraction process.

The technique uses an energy minimization framework. A contour has two energy functions associated with it: an internal and an external energy. The internal energy measures desired properties of a contour's shape, such as smoothness and continuity. The external energy is derived from a selected image functional, to measure desired features such as edges, lines, regions [14] and, recently, texture [9]. The internal energy, the a priori information, regularises the external energy [18], the a posteriori information. The technique refines an estimated initial contour by an energy minimization technique.

The original technique [10] defines the snake energy,  $E_{snake}$ , of a contour,  $\mathbf{v}$ , to be

$$E_{snake}(\mathbf{v}(s)) = \int_{s=0}^1 \alpha(s) \left| \frac{d\mathbf{v}}{ds} \right|^2 + \beta(s) \left| \frac{d^2\mathbf{v}}{ds^2} \right|^2 - \gamma |\nabla I(\mathbf{v})| ds \quad (1)$$

where the first two internal energy terms measure the continuity and smoothness, respectively, and the last is an external term characterising an edge by a high gradient of the image  $I$ ;  $\alpha$ ,  $\beta$ , and  $\gamma$  are the associated weighting parameters. The technique requires the initial contour to lie outside the feature of interest and relies on an inherent contraction force to move the contour towards the feature. Cohen [2] proposed an inflating contour that reduced the sensitivity to initialization, but increased the number of parameters. Berger [1] proposed a, similar, expanding contour. These techniques are constrained by their gradient descent nature, with a

solution that is highly dependent on the initial contour due to many local minima within a typical external energy function. Use of simulated annealing for minimization [17], and dynamic programming [5] have been proposed to reduce problems caused by local minima. However, these techniques are restricted by difficulty in choosing appropriate parameters due to scale variance and parameter interdependence. Furthermore, a conventional snake's inherent contraction force compounds the parameter problem and makes the generalization to open contours difficult. Alternative approaches to the problem of initialization can use exhaustive initializations [19], [21], but their computationally expensive nature is not justified for many applications. The generalised Hough transform has recently been used [11] to provide initial contours when substantial prior knowledge is available.

Here, we introduce a new dual active contour that confronts the two primary problems of initialization and parameterization. The technique uses two contours to search the image space: one which contracts from outside an initial estimate, and one which expands from inside. This reduces the sensitivity to initialization, by enabling a comparison between the contours' energy, which is used to objectively reject weak minima, as advocated earlier [4]. The scale-variance of the internal energy function in a conventional snake makes it difficult to compare the behaviour of contracting and expanding contours. This also illustrates the main difficulty in determining appropriate values for the parameters. To overcome difficulty in this choice, and to enable a comparison between contours, we develop a scale invariant internal energy function [6], that retains the conventional continuity and smoothness constraints, but removes the unwanted contraction force. The new contour has no preference to expand or contract, other than to acquire its natural shape. This is similar to a recent approach which removed the contraction force [20], but it is more efficient by the use of a direct implementation, and moreover it enables prior shape information to be integrated within the contour. This is achieved by a simple relationship between the local geometry of the contour and its internal parameters. The contraction force is replaced with an adaptive driving force that allows the technique to search for a good minimum. The dual technique is controlled by two independent parameters: a regularization parameter which controls the trade-off between the internal energy and the external energy, and a resolution parameter which places a lower limit on the energy minimum at which evolution is halted.

First, we will introduce the original energy minimization technique, and then develop the dual minimization technique, showing how it overcomes the main problems. Finally we apply the technique to synthetic and real image data, using open and closed contour configurations.

## 2 ENERGY MINIMIZATION

To illustrate the problems associated with gradient descent minimization, combined with the contraction force, we consider the energy function shown in Fig. 1, considering it to be a radial slice through a circularly symmetric image function. Using a concentric circular initialization, symmetry allows us to reduce the problem to one dimension, the contour retains its circularity and shrinks as it evolves. A non-trivial solution depends on whether the image forces can support the contracting internal forces. By symmetry, the internal force  $F$  acting on a point on the contour can be derived from the evolution equation in [10] and is given by,

$$F \approx R \frac{\tau(4\pi^2\alpha + 16\pi^4\beta)}{1 + \tau(4\pi^2\alpha + 16\pi^4\beta)} \quad (2)$$

where  $R$  is the radius and  $\tau$  is the time step. It is evident that the

• The authors are with the ISIS research group, Dept. of Electronics and Computer Science, University of Southampton, U.K, SO17 1BJ.  
E-mail: {srg, msn}@rz.uni-jena.de.

Manuscript received May 154, 1995; revised Oct. 1, 1996. Recommended for acceptance by B. Vemuri.

For information on obtaining reprints of this article, please send e-mail to: [transpami@computer.org](mailto:transpami@computer.org), and reference IEEECS Log Number P96106.

internal force is not scale invariant: as the contour shrinks the force decreases. Furthermore the force is not linearly dependent upon the time step, and therefore the time step not only controls the stability of the evolution but also governs the solution. The contraction force will displace the solution from a minimum because it requires an image gradient to bring it into equilibrium. Therefore, depending on the choice of parameters it is possible to obtain any of the three solution regions shown in Fig. 1 (solutions in the range 2-3, 4-5, and 6 inward). However, the shape of the energy function is not known a priori, and therefore it is impossible to determine a set of parameters to obtain a "good" solution, such as minimum 0.4 in Fig. 1.

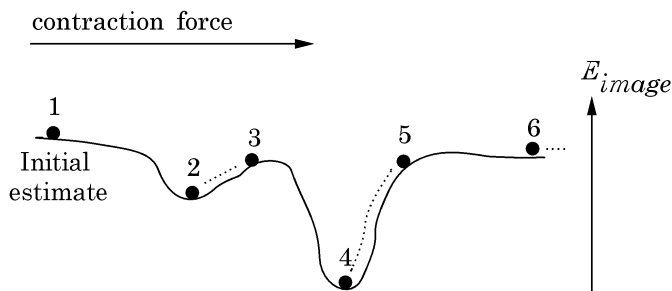


Fig. 1. Energy minimization.

To overcome this problem we remove the contraction term from the contour which removes any tendency to expand or contract. The corresponding solution in Fig. 1 is point 2, the nearest minimum. However the contour is now sensitive to local minima and consequently sensitive to initialization. A strategy which finds a "good" minimum is now required. Accordingly, we use two contours [7], one inside and one outside the feature of interest. The two contours aim to find a local energy minimum according to a trade-off between the prior shape constraints and the image. When both contours become stationary, the contour with the highest energy is minimized with an additional force pushing it towards the other, which is obtained using an arc length correspondence. This equips the contours with a hill climbing ability to escape from weak local minima. If the energy of the contour drops below the other we remove the driving force and let it find a better minimum. The driving force is now applied to the other contour and the process repeats until both contours have found the same solution. By using two contours approaching the feature from either side we provide a more balanced technique, whose ability to reject weak local minima increases its robustness. Accordingly the solution must lie within the specified region of interest, but uncertainty in the initial estimate can be accommodated by varying the initialization region and hence the search space.

One difficulty with constant normal driven techniques [2], [20] is that the driving force increases difficulty in parameter determination. If the driving force is too high the contour will be driven over the feature of interest, if it is too low it may become entrapped in a weak local minimum. In order to avoid this, we advocate the use of an adaptive force that takes into account the energy of both contours and the rate at which the contour currently being minimized is moving. The new driving force pushes the contour with the highest energy into a lower energy state. We retain a global force for simplicity, but use its adaptive nature to move the parts of the contour in the weakest minimum first. The greedy nature of the minimization technique implies that a global minimum is no longer guaranteed when the technique is generalised to the two dimensional case.

A steepest gradient descent method does not generally have a finite convergence. Consequently it is necessary to apply a crite-

riion to terminate the evolution. A suitable criterion uses a termination parameter,  $\delta$  which is related to the rate of a snake's evolution

$$\max_i |\mathbf{v}_i^{t+1} - \mathbf{v}_i^t| < \delta \quad (3)$$

This controls the driving force adaptively. If the total energy of the currently selected contour is higher than the other, the force is increased until the contour passes the termination criterion. This guarantees that a part of the contour is moving at a rate controlled by  $\delta$ . Meanwhile if the energy begins to decrease, the driving force is removed and the contour is allowed to come into equilibrium. The process repeats until both contours have found the same equilibrium. The rate of evolution of the contour, which controls the spatial resolution of our technique, is determined by  $\delta$ .

### 3 SNAKE FORMULATION AND IMPLEMENTATION

#### 3.1 Local Shape Model

A single contour can be formulated to allow local shape information to be integrated within it [11]; two such contours are used within the dual technique. The internal energies of the two contours are required to be scale, rotation and translation invariant so that contours may be compared. This enforces a balanced evolution of the contracting outer contour and the expanding inner contour. The contour should have an equilibrium when it is similar to an estimated contour so that it has no preference to expand or contract, other than to acquire its natural shape.

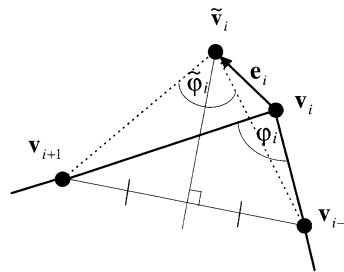


Fig. 2. Local shape model.

The original technique implements the internal continuity and smoothness constraints by two regularising functions [18], which effectively low-pass filter the contour. These result in contraction [8]: Closed and open contours shrink to a point without the support of external forces. Modification of the continuity and curvature constraints to remove the unwanted contraction force, produces a solution that is insensitive to the internal parameters [20], and provides no prejudice towards expansion or contraction, as required. To implement these properties we impose two constraints. Using a discrete contour which is a set of points  $\mathbf{v}_i = (x_i, y_i)$  for  $i = 0 \dots N-1$ , where  $N$  is the number of points. All subscript arithmetic is modulo  $N$  for closed contours, and contours are described in an anti-clockwise manner. To ensure that contour points are evenly spaced we impose the condition

$$|\mathbf{v}_{i-1} - \mathbf{v}_i| = |\mathbf{v}_{i+1} - \mathbf{v}_i| \quad (4)$$

A second condition causes the contour to take a specified shape. In the case of a circle,

$$\varphi_i = \frac{(N-2)\pi}{N} \quad (5)$$

where  $\varphi$  is the internal angle, the tangent angle at the contour points. These two conditions are applied by a force that pulls  $\mathbf{v}_i$  towards its estimated position,  $\tilde{\mathbf{v}}_i$ , Fig. 2. This force,  $\mathbf{e}_i$ , is calculated from the neighboring points of  $\mathbf{v}_i$  by,

$$\mathbf{e}_i = \tilde{\mathbf{v}}_i - \mathbf{v}_i = \frac{1}{2}(\mathbf{v}_{i-1} + \mathbf{v}_{i+1}) - \mathbf{v}_i + \theta_i \frac{1}{2} \mathbf{R}(\mathbf{v}_{i-1} - \mathbf{v}_{i+1}) \quad (6)$$

where  $\mathbf{R}$  is a  $+90^\circ$  rotation matrix and  $\theta$  is related to the local tangent angle. The internal energy of the contour at  $\mathbf{v}_i$  is the energy associated with the force  $\mathbf{e}$ , normalised by the average space step,  $h$ , rendering the energy scale invariant (Appendix: Lemma 1), giving the local energy  $E_{lshape}$  as

$$E_{lshape}(\mathbf{v}_i) = \frac{1}{2} \left( \frac{|\mathbf{e}_i|}{h} \right)^2 \quad (7)$$

The internal energy term, (7), is locally isotropic which is desirable whereas the original snake's internal energy generally was not. The value of  $\theta$  is related to the internal angle  $\varphi$  by,

$$\theta = \cot\left(\frac{\varphi}{2}\right) \quad (8)$$

If there are  $N$  points then the discrete contour is an  $N$ -sided polygon. From (5)

$$\theta = \cot\left(\frac{(N-2)\pi}{2N}\right) = \tan\left(\frac{\pi}{N}\right) \quad (9)$$

will cause the contour to assume the shape of a (discrete) circle. This circle is a global solution to the internal energy. The contour will have a non-trivial equilibrium provided it does not expand (or contract) indefinitely, which is possible provided:

$$\sum_{i=0}^{N-1} \varphi_i = (N-2)\pi \quad \text{and} \quad 0 < \varphi_i < 2\pi \quad (10)$$

Including higher level shape information, [12], [16], other than low overall curvature can be advantageous. The local shape model allows such information to be integrated within the contour, by modifying the values of  $\theta$ , to change the contour's natural shape. Hence our new formulation allows any estimate of shape to be included as an equilibrium state. Negative values of  $\theta$  can cause the contour to become concave. However, to fully exploit this additional shape information it is necessary to have an estimate of a feature's orientation. The complete contour energy equation is given by,

$$E_{snake}(\mathbf{v}) = \frac{1}{N} \sum_{i=0}^{N-1} \lambda E_{lshape}(\mathbf{v}_i) + (1-\lambda) E_{ext}(\mathbf{v}_i) \quad (11)$$

This form emphasises the original paradigm of regularization [11]; the only parameter to be chosen is the regularization parameter,  $\lambda$ , which lies between 0 and 1. If  $\lambda = 1$  the contour is completely regularised and depends only on internal forces for its solution, in which case the contour will assume the local shape specified by the two conditions (4) and (5). If  $\lambda = 0$  then the contour is not regularised and no constraints on the contour's shape or continuity are applied, the contour terminates at a minimum associated with the chosen image functional.

Generalising the original technique to open contours is difficult since the elasticity constraint can shrink an open contour to a point. Our internal energy does not admit such problems and an open contour can be created by removing the internal energy from the two end points.

### 3.2 Minimization

The dual approach takes the inner and outer estimated contours and evolves them according to the following algorithm. Having selected the contour with the highest energy (11), if its movement remains below the termination condition (3) the driving force is increased until it moves at a rate greater than the chosen threshold,  $\delta$ . When the energy begins to decrease, the added driving force is removed and the contour is allowed to come into equilibrium.

The procedure is then repeated until both contours have found the same equilibrium, which is guaranteed by the direction of the driving force.

### 3.3 Implementation

The minimization process is implemented by the method of gradient descent. The rate of evolution controls the stability and convergence of the minimization process [15]. The evolution must be controlled to ensure that a contour cannot move by more than one pixel, in one iteration, ensuring stability and consideration of all appropriate image data. The external forces,  $\mathbf{F}$ , are derived from the external image energy  $E_{ext}$ .

$$\mathbf{F}_i = -k \begin{pmatrix} \frac{\partial E_{ext}}{\partial x} \Big|_{\mathbf{v}_i} \\ \frac{\partial E_{ext}}{\partial y} \Big|_{\mathbf{v}_i} \end{pmatrix} \quad (12)$$

Bilinear interpolation [3] ensures that a stable convergence is attainable. The constant,  $k$ , is chosen to normalise the external forces so that they lie within the interval  $[-1, 1]$ . Then the contour,  $\mathbf{v}$ , is evolved according to,

$$\mathbf{v}_i^{t+1} = \mathbf{v}_i^t + \frac{1}{2} \left( \lambda \frac{\mathbf{e}_i}{h} + (1-\lambda) \mathbf{F}_i \right) + g(t) \frac{\mathbf{u}_i - \mathbf{v}_i^t}{|\mathbf{u}_i - \mathbf{v}_i^t|} \quad (13)$$

where  $\mathbf{u}$  is the other contour and  $g(t)$  is the strength of the adaptive driving force, which is modified by the minimization algorithm. This evolution equation ensures the rate of evolution is scale invariant and lies within one pixel (Appendix: Lemma 2).

## 4 RESULTS

To demonstrate performance, the new technique is compared with a conventional single Kass snake [10] and the robust snake of Xu [20], using synthetic and real images. The image functionals used in the tests were the edge-based  $E_{ext}(\mathbf{v}) = -|\nabla I(\mathbf{v})|$ . To evaluate the performance in the presence of noise, a simulation used a circle with zero mean additive Gaussian noise using a unit image contrast. For the synthetic images, the contours are initialized at many randomly selected positions, within and without the target circle. The external contour for the dual snake was used as the initial contour for the techniques of Kass and Xu. The regularization parameter for the dual technique determines the trade-off between the prior shape information and the image data. A low regularization causes the image forces to dominate the shape constraints and the contour adheres to the image data well. However in the presence of noise we require a greater emphasis on the shape constraints and hence a greater regularization. In between these extrema, we require a trade-off between accurate representation to the data and accurate representation to the prior shape constraints. For the dual technique  $\lambda = 0.5$  was used. The termination parameter is chosen to be a fraction of the pixel size and hence  $\delta = 0.05$  was used. The local shape parameter,  $\theta$ , was set to the circular case, (5). In order to find sets of parameters for the Xu and Kass techniques which gave good results, many trial runs were performed and a manually optimised set of parameters were determined. The approach of Xu was modified since the least squares fitting in the removal of the contraction [20] can become unstable when the points are nearly collinear. A line was also fitted and if this was a better fit than a circle, the curvature was taken to be zero.

To assess similarity between two contours  $\mathbf{u}$  and  $\mathbf{v}$ , we used the Euclidean feature distance  $d(\mathbf{u}, \mathbf{v})$  of the contours' Fourier Descriptors [13],  $\mu$  and  $\nu$ ,

$$d(\mathbf{u}, \mathbf{v}) = \left[ \sum_{n=-M}^M |\mu_n - v_n|^2 \right]^{\frac{1}{2}} \quad (14)$$

which is equivalent to measuring the mean-square deviation between the contours. Example results are shown in Fig. 3 for the techniques applied to the cup image and in Fig. 4 applied to the simulation data. The aim was to extract the cup rim and the circle in the simulation data. The example results confirm that the dual contour can select the chosen target.

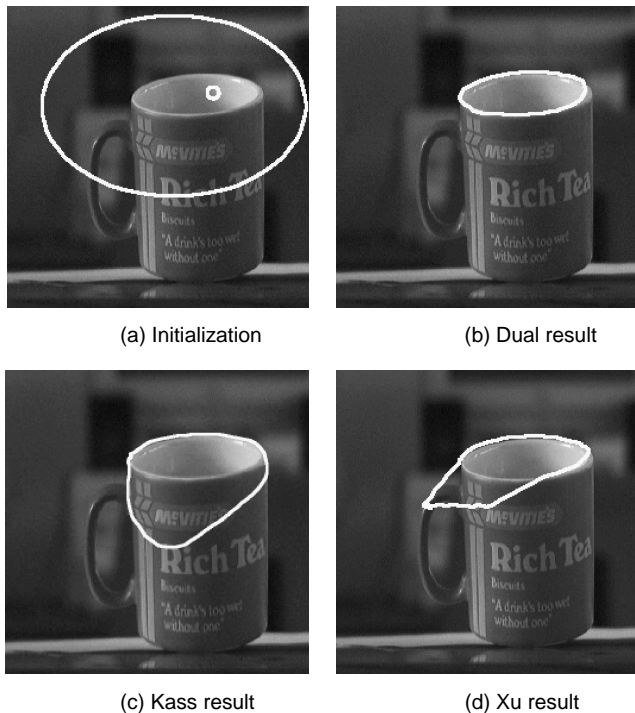


Fig. 3. Cup example.

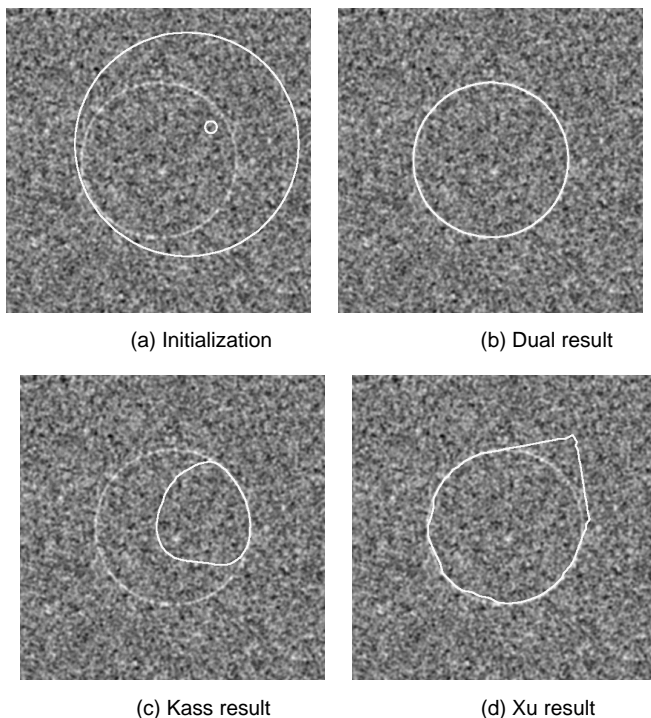


Fig. 4. Noise example.

The cup image illustrates the advantage of approaching a feature from both sides. As a consequence of the initialization, Fig. 3a and the parameters used, the Kass technique, Fig. 3c, and Xu technique, Fig. 3d, become snagged on complex image data, whereas the dual technique is able to reject such minima, Fig. 3b. This allows much greater freedom in deployment; the dual contour guarantees a good result within the region specified by the initial contours. Its formulation ensures that this is achieved without a lengthy manual optimization of its parameters.

For the synthetic data, for ten initializations for each image, the dual technique performed better, working well in up to a noise standard deviation of 1.2, Fig. 4b. In contrast, the techniques of Kass and Xu, (both initialized with the outer contour, Fig. 4a) could and did select the target in some cases of the simulation data, but failed for cases of poor initialization and increased noise. The example shown in Fig. 4c demonstrates the problem associated with the scale variant internal forces for the Kass snake. To achieve good results in the presence of high noise requires a high regularization. The part of the initial contour that lies near the circle edge is driven over it, but the part which is farthest away stops at the circle. This is a consequence of the internal forces decreasing as the contour shrinks. The Xu technique is able to form corners, Fig. 4d, as a result of the removal of the contraction force, accounting for poorer overall performance for the synthetic data. The dual technique enforces the local shape regularization and avoids this problem. Table 1 gives an average measure of the mean square error against the noise standard deviation, for the three techniques. It can be seen that the performance of the dual technique is superior to the single snake approaches because the performance reduces less when the noise standard deviation increases. The threshold, at which performance deteriorates, is higher for the dual contour which demonstrates an ability to handle greater noise degradation. However, if the Kass and Xu snake parameters used here are now applied to other images, with different depths of minima, the single snake may fail to be attracted by them or be attracted to insignificant local minima. On the other hand, the dual technique—by virtue of its adaptive driving force—is sufficiently sensitive to extract different degrees of minima without the need to modify its parameters.

TABLE 1  
RESULTS OF MSE AGAINST NOISE STANDARD DEVIATION

Noise STD	0.0	0.4	0.8	1.2	1.6	2.0
Kass	0.31	0.44	0.70	22.6	23.8	40.0
Xu	1.25	1.50	10.6	36.1	34.1	42.9
dual	0.12	0.19	0.29	2.82	19.5	38.4

## 5 CONCLUSIONS

In this paper, we have developed a comprehensive dual contour technique that overcomes the primary problems of sensitivity to initialization and parameters associated with the original techniques. This sensitivity is a consequence of the formulation of the original techniques in searching for a minimum. Typically, there are many local minima and consequently the solution is highly dependent upon the choice of parameters and initial contour. We have proposed a new criterion in searching for a good minimum within the region specified by two initial contours. This is made possible by a reformulated internal energy which renders the snake energy scale invariant and provides a basis for assessing the merits of solutions. The original technique used the internal forces to provide a contraction of the contour, to move it towards features. This increased the sensitivity to the parameters and therefore we removed the contraction force from the internal constraints. The contraction force is replaced with a new adaptive

driving force which allows the contour to find minima, and to escape from them if a better solution has been found by the other contour. Furthermore if shape information and orientation are available, our technique is able to exploit this by integration within the internal energy function. The results demonstrate that the new technique can provide good performance over images from different sources, with the same parameters.

## APPENDIX—SNAKE PROPERTIES

A translation, rotation and scale transformation can be defined as,

$$\mathbf{U} = \mathcal{S} \begin{pmatrix} \cos \theta & -\sin \theta \\ \sin \theta & \cos \theta \end{pmatrix} \mathbf{V} + \begin{pmatrix} x_{\text{offset}} \\ y_{\text{offset}} \end{pmatrix} = \mathbf{A}\mathbf{V} + \mathbf{B} \quad (15)$$

Let  $h$  be the step size and it is assumed to be constant over one iteration. This is justified by the techniques promotion of an evenly spaced set of points.

**LEMMA 1.** *The local shape energy,  $E_{\text{shape}}$ , is scale, translation and rotation invariant.*

**PROOF.** From (6) and (7), the local shape energy for a contour  $\mathbf{U}$  is,

$$E_{\text{shape}}(\mathbf{U}_i) = \frac{1}{8} \frac{|\mathbf{U}_{i-1} - 2\mathbf{U}_i + \mathbf{U}_{i+1} + \theta_i \mathbf{R}(\mathbf{U}_{i-1} - \mathbf{U}_{i+1})|^2}{h^2} \quad (16)$$

Using (15) and  $h = |\mathbf{U}_i - \mathbf{U}_{i-1}| = |\mathbf{U}_i - \mathbf{U}_{i+1}|$  gives

$$= \frac{1}{8} \frac{|\mathbf{A}(\mathbf{V}_{i-1} - 2\mathbf{V}_i + \mathbf{V}_{i+1} + \theta_i \mathbf{A}^{-1} \mathbf{R} \mathbf{A}(\mathbf{V}_{i-1} - \mathbf{V}_{i+1}))|^2}{|\mathbf{A}(\mathbf{V}_i - \mathbf{V}_{i-1})|^2} \quad (17)$$

Since  $\mathbf{A}^{-1} \mathbf{R} \mathbf{A} = \mathbf{R}$

$$= \frac{1}{8} \frac{|\mathbf{A}(\mathbf{V}_{i-1} - 2\mathbf{V}_i + \mathbf{V}_{i+1} + \theta_i \mathbf{R}(\mathbf{V}_{i-1} - \mathbf{V}_{i+1}))|^2}{|\mathbf{A}(\mathbf{V}_i - \mathbf{V}_{i-1})|^2} = E_{\text{shape}}(\mathbf{V}_i) \quad (18)$$

Hence the energy of the transformed contour equals the energy of the original contour.  $\square$

**LEMMA 2.** *The evolution of the local shape contour is scale invariant.*

**PROOF.** Since the external forces are independent of the contour's scale it is only necessary to show the evolution is invariant for the internal forces. The evolution equation, (13), for the internal forces gives

$$\mathbf{U}_i^{t+1} - \mathbf{U}_i^t = \frac{1}{2} \left( \lambda \frac{\mathbf{e}_i}{h} \right) \quad (19)$$

From (6),

$$\mathbf{U}_i^{t+1} - \mathbf{U}_i^t = \frac{1}{2} \left( \lambda \frac{1}{2} \frac{(\mathbf{U}_{i-1} - 2\mathbf{U}_i + \mathbf{U}_{i+1} + \theta_i \mathbf{R}(\mathbf{U}_{i-1} - \mathbf{U}_{i+1}))}{h} \right) \quad (20)$$

Using (15) gives

$$= \frac{\lambda}{4} \frac{\mathbf{A}(\mathbf{V}_{i-1} - 2\mathbf{V}_i + \mathbf{V}_{i+1} + \theta_i \mathbf{A}^{-1} \mathbf{R} \mathbf{A}(\mathbf{V}_{i-1} - \mathbf{V}_{i+1}))}{\mathbf{A}(\mathbf{V}_i - \mathbf{V}_{i-1})} \quad (21)$$

Since  $\mathbf{A}^{-1} \mathbf{R} \mathbf{A} = \mathbf{R}$

$$= \frac{\lambda}{4} \frac{(\mathbf{V}_{i-1} - 2\mathbf{V}_i + \mathbf{V}_{i+1} + \theta_i \mathbf{R}(\mathbf{V}_{i-1} - \mathbf{V}_{i+1}))}{(\mathbf{V}_i - \mathbf{V}_{i-1})} = \mathbf{V}_i^{t+1} - \mathbf{V}_i^t \quad (22)$$

Hence the evolution of the transformed contour equals the evolution of the original contour.  $\square$

## ACKNOWLEDGMENTS

Steve Gunn gratefully acknowledges tenure of an EPSRC research studentship. The authors would also like to thank the referees for their perceptive comments.

## REFERENCES

- [1] M.O. Berger, "Towards Dynamic Adaption of Snake Contours," *Proc. Sixth Int'l Conf. Image Analysis and Processing: Progress in Image Analysis and Processing II*, pp. 47-54, Como, Italy, 1991.
- [2] L.D. Cohen and I. Cohen, "Finite-Element Methods for Active Contour Models and Balloons for 2D and 3D Images," *Trans. Pattern Analysis and Machine Intelligence*, vol. 15, no. 11, pp. 1131-1147, 1993.
- [3] L.D. Cohen, "Note: On Active Contour Models and Balloons," *CVGIP: Image Understanding*, vol. 53, no. 2, pp. 211-218, 1991.
- [4] P. Fua and Y.G. Leclerc, "Model Driven Edge Detection," *Machine Vision and Applications*, vol. 3, pp. 45-56, 1990.
- [5] D. Geiger, A. Gupta, L.A. Costa, and J. Vlontzos, "Dynamical Programming for Detecting, Tracking and Matching Deformable Contours," *Trans. Pattern Analysis and Machine Intelligence*, vol. 17, no. 3, pp. 294-302, 1995.
- [6] S.R. Gunn and M.S. Nixon, "Improving Snake Performance Via a Dual Active Contour," *Lecture Notes in Computer Science*, vol. 670, pp. 600-605, 1995.
- [7] S.R. Gunn and M.S. Nixon, "A Dual Active Contour," *Proc. BMVC 94*, pp. 305-314, York, U.K., Sept., 1994.
- [8] B.K. Horn and E.J. Weldon, "Filtering Closed Curves," *Trans. Pattern Analysis and Machine Intelligence*, vol. 21, no. 3, pp. 269-281, 1972.
- [9] J. Ivins and J. Porrill, "Active Region Models for Segmenting Textures and Colours," *Image and Vision Computing*, vol. 13, no. 5, pp. 431-438, 1994.
- [10] M. Kass, A. Witkin, and D. Terzopoulos, "Snakes: Active Contour Models," *Int'l J. Computer Vision*, vol. 1, pp. 321-331, 1988.
- [11] K.F. Lai and R.T. Chin, "Deformable Contours—Modeling and Extraction," *Trans. Pattern Analysis and Machine Intelligence*, vol. 17, no. 11, pp. 1,084-1,090, 1995.
- [12] S. Menet, P. Saint-Marc, and G. Medioni, "Active Contour Models: Overview, Implementation and Applications," *Int'l Conf. Systems, Man, and Cybernetics*, vol. 212, pp. 194-199, 1990.
- [13] E. Persoon and K.S. Fu, "Shape Discrimination Using Fourier Descriptors," *Trans. Systems, Man, and Cybernetics*, vol. 7, no. 3, pp. 170-179, 1977.
- [14] R. Ronfard, "Region-Based Strategies for Active Contour Models," *Int'l J. Computer Vision*, vol. 13, no. 2, pp. 229-251, 1994.
- [15] N. Rougon, "Kinematics of Interface Evolution with Application to Active Contour Models," *SPIE Curves and Surfaces in Computer Vision and Graphics II*, vol. 1,610, pp. 336-348, 1991.
- [16] L.H. Staib and J.S. Duncan, "Boundary Finding with Parametrically Deformable Models," *Trans. Pattern Analysis and Machine Intelligence*, vol. 14, no. 11, pp. 1061-1075, 1992.
- [17] G. Storvik, "A Bayesian Approach to Dynamic Contours through Stochastic Sampling and Simulated Annealing," *Trans. Pattern Analysis and Machine Intelligence*, vol. 16, no. 10, pp. 976-986, 1994.
- [18] D. Terzopoulos, "Regularization of Inverse Visual Problems involving Discontinuities," *Trans. Pattern Analysis and Machine Intelligence*, vol. 8, no. 4, pp. 413-424, 1986.
- [19] Y. Wang and O. Lee, "Active Mesh—A Feature Seeking and Tracking Image Sequence Representation Scheme," *Trans. Image Processing*, vol. 3, no. 5, pp. 610-624, 1994.
- [20] G. Xu, E. Segawa, and S. Tsuji, "Robust Active Contours with Insensitive Parameters," *Pattern Recognition*, vol. 27, no. 7, pp. 879-884, 1994.
- [21] S.W. Zucker, C. David, A. Dobbins, and L. Iverson, "The Organization of Curve Detection: Coarse Tangent Fields and Thin Spline Coverings," *Proc. Second Int'l Conf. Computer Vision*, pp. 568-577, Tampa, Fla., Dec. 1988.